

~~70-2738~~

X-551-70-122

PREPRINT

N70-27385
FMX-63908

DETECTION OF RANGE RATE BIAS IN THE TWO-WAY DOPPLER MEASUREMENTS OF EXPLORER 34

C.W. Murray, Jr.

CASE FILE COPY

April 1970



GODDARD SPACE FLIGHT CENTER
GREENBELT, MARYLAND

X-551-70-122
PREPRINT

DETECTION OF RANGE RATE BIAS IN THE
TWO-WAY DOPPLER MEASUREMENTS
OF EXPLORER 34

C. W. Murray, Jr.

April 1970

GODDARD SPACE FLIGHT CENTER
Greenbelt, Maryland

DETECTION OF RANGE RATE BIAS IN THE
TWO-WAY DOPPLER MEASUREMENTS
OF EXPLORER 34

C. W. Murray, Jr.

ABSTRACT

A bias of a few centimeters per second in the two-way Doppler range rate measurements of Explorer 34 has been detected through orbit determination techniques. Results of a previous theoretical analysis indicate that a 3 centimeter per second bias can be attributed to the effect of satellite spin on the measurements.

This paper verifies the previous analysis and shows that by "correcting" the range rate data for this bias, the total weighted root mean square of the residuals after fit by the equations of motion is reduced.

A discussion of Maximum Likelihood Estimation in the orbit determination process and optimum statistical properties of the estimator is also included.

SUMMARY

A bias of a few centimeters per second in the two-way Doppler range rate measurements of Explorer 34 has been detected using orbit determination techniques. Results of a previous theoretical analysis indicate that a 3 centimeter per second bias can be attributed to the effect of satellite spin on the measurements. In the case of Explorer 34 the turnstile antenna elements were connected to give a different polarization on receive than on transmit. If the antenna connections were such as to result in the same polarization for both transmit and receive, the magnitude of the effect would have been increased and a bias on the order of a meter/second would have resulted.

The results of this analysis verify the bias in the range rate measurements due to the effect of satellite spin in the sense that the rms of fit was reduced when a "correction" of opposite sign to the bias was added to all the range rate measurements and the state vector of the satellite at epoch solved for using orbit determination techniques.

The effect of a bias of a few centimeters per second on the orbit of Explorer 34 is investigated and it is shown that a 6 centimeter per second bias when added to the range rate measurements produces an rss error in position on the order of a half a kilometer and an rss error in velocity on the order of 1 to 2 centimeters per second when averaged over the same time period as the data arc.

For two of the data arcs used in the analysis a bias of approximately 6 centimeters per second was "solved for" and for the third arc a bias of 2.5 centimeters per second was "solved for" by orbit determination techniques. Since there were no ionospheric corrections made within the program it is felt that the difference between the bias as predicted due to the spin and that "solved for" can be attributed to the effects of the ionosphere.

A discussion of Maximum Likelihood Estimation in the orbit determination process and optimum statistical properties of the estimator is also included.

CONTENTS

	<u>Page</u>
ABSTRACT	iii
SUMMARY	iv
INTRODUCTION	1
THE BIAS IN RANGE RATE MEASUREMENTS DUE TO SATELLITE SPIN	3
THE EXPECTED RANGE RATE BIAS DUE TO SATELLITE SPIN FOR EXPLORER 34.....	6
SOLUTION FOR RANGE RATE BIAS USING ORBIT DETERMINATION TECHNIQUES	8
THE EFFECT OF RANGE RATE BIAS ON THE ORBIT AND RMS POSITION AND VELOCITY ERRORS OF EXPLORER 34.....	9
DISCUSSION.....	13
CONCLUSIONS	18
ACKNOWLEDGMENTS	19
REFERENCES	19
APPENDIX A — THE ANTENNA CONNECTIONS ON EXPLORER 34	A-1
APPENDIX B — MAXIMUM LIKELIHOOD ESTIMATION IN THE ORBIT DETERMINATION PROCESS	B-1
GLOSSARY AND DEFINITION OF SYMBOLS	B-13
APPENDIX C — DEFINITION OF COORDINATE SYSTEM AND RADIAL, CROSS TRACK AND DOWN TRACK UNIT VECTORS.....	C-1

ILLUSTRATIONS

<u>Figure</u>		<u>Page</u>
1	Turnstile Antenna Rotating in a Right-Handed Sense About the Positive z-axis, and Radiating a Right Hand Circularly Polarized Wave Along This Axis	5
2	Geometrical Configuration of Explorer 34	7
3	Total Weighted RMS vs Range Rate Bias — Explorer 34 Epoch, 26 August '68 13 ^h 55 ^m GMT	10
4	Total Weighted RMS vs Range Rate Bias — Explorer 34 Epoch, 30 August 1968 13 ^h 55 ^m GMT	11
5	Total Weighted RMS vs Range Rate Bias — Explorer 34 Epoch, 13 December 1968 15 ^h 21 ^m GMT	12
A-1	Explorer 34 Satellite	A-2
A-2	Explorer 34 Feed System	A-3
A-3	Relative Phase of Monopoles at Reference Time t_0 (Transmit) .	A-4
A-4	Current Flow at Time t_0 (Transmit) Under Dipole Representation	A-4
A-5	Current Flow at Some Time Later (Transmit) Under Dipole Representation	A-4
A-6	Current Flow at Some Reference Time t_0 (Receive) Under Dipole Representation	A-5
A-7	Current Flow at Some Later Time (Receive) Under Dipole Representation	A-5
C-1	Inertial Coordinate System.....	C-2
C-2	Radial, Along Track, and Cross Track Unit Vectors In Terms of \vec{R} and \vec{V}	C-3

TABLES

<u>Table</u>		<u>Page</u>
1	Effect of a Fixed Bias of +6 Centimeters/Second and -6 Centimeters/Second in Range Rate Upon the Orbit of Explorer 34.....	14

DETECTION OF RANGE RATE BIAS IN THE
TWO-WAY DOPPLER MEASUREMENTS
OF EXPLORER 34

INTRODUCTION

Spin stabilization is one of the methods for controlling the attitude of a spacecraft, i.e., its orientation with respect to some reference frame. By this technique one of the body axes is fixed in inertial space while the satellite rotates around it.

Since their aspect is continually changing as viewed from the earth, spin-stabilized satellites usually require an omnidirectional type antenna system. The turnstile antenna is omnidirectional, and, in addition, is simple and practical. It is therefore used on many spin-stabilized satellites (Reference 1).

In Reference 2 it is shown that the phase pattern of a turnstile antenna can be expressed as a linear function plus a periodic function of the angle of rotation. As the satellite spins the varying phase pattern introduces both a bias and fluctuations (related to harmonics of the spin rate) in the two-way Doppler (the time rate of change of the phase of the carrier frequency) range-rate measurements. The bias results from the linear term while the harmonics of the spin rate result from the periodic terms. Reference 2 is mainly concerned with the fluctuations in the two-way Doppler data taken on Explorer 33 and 35.* It is shown that due to both physical and electrical symmetry the even harmonics predominate. In addition the spin rate can be determined in a least squares sense by fitting a

*Both Explorer 33 and 35 employ a canted turnstile antenna which is located symmetrically with respect to the spin axis and both operate at VHF for purposes of obtaining range and range rate information.

non-linear model to the data. When this is done the rms of the residuals is reduced by a factor of 1/2 to 1/3 compared to the rms of the residuals from a least squares straight line fitted to the same data.

Marini (Reference 3) considers the bias effect on two-way Doppler range-rate measurements due to the rotation of a spin-stabilized satellite employing a turnstile antenna for reception and retransmission. He discusses two different types of tracking systems that employ coherent two-way Doppler measurement of range rate (Goddard Range and Range Rate System and the Unified S-Band System used to track Apollo spacecraft), and in both systems the range rate measurement is changed by the amount

$$\Delta \dot{r} = \frac{s_r + s_t / (k)}{2} \lambda_t f_s$$

where k is the turn-around ratio of the satellite transponder, λ_t is the wavelength of the ground-based transmitter, and f_s is the spin rate of the satellite. The symbols s_r and s_t are plus or minus one according to the sense of the spin and polarization of the satellite receive and transmit antennas.

The purpose of the present paper is two-fold: (1) to verify through orbit determination techniques a bias of several centimeters per second in the two-way Doppler range rate measurements of Explorer 34 (IMP-4)* which can be attributed to the spin of the satellite as predicted in the theoretical analysis in Reference 3, and; (2) to show the effect of a fixed bias in range rate on the orbit and rms position and velocity errors of the satellite.

*Explorer 34, like Explorers 33 and 35, is spin-stabilized, employing a turnstile antenna for reception and retransmission, and operating at VHF for ranging and range rate information.

Explorer 34 was launched on 24 May 1968. It reentered the atmosphere and crashed on 3 May 1969. For the time period covering this analysis, the satellite was in an elliptical orbit about the earth with the following approximate Keplerian elements:

Semi-major axis	112,000 km
Eccentricity	0.91
Inclination	70°
Right Ascension of the Ascending Node	165°
Argument of Perigee	190°

Its period was approximately 4 days.

THE BIAS IN RANGE RATE MEASUREMENTS DUE TO SATELLITE SPIN

The following discussion can be found in Reference 3. It is repeated here for purposes of completeness.

In Reference 3 it is shown that for the Goddard Range and Range Rate System which employs a coherent two-way Doppler measurement of range rate, in the case of a spinning satellite with a turnstile antenna, processing by the ground-based receiver will produce an output frequency (see Equation 18 of Reference 3)

$$f_o = (k_u k_d - 1) f_t + \frac{k_d (s_r + s_t (N/M)) f_s}{1 + (r/c)} + f_b \quad (1)$$

where k_u and k_d are the uplink and downlink Doppler factors whose product is given by (Reference 4)

$$k_u k_d = \frac{1 - \dot{r}/c}{1 + \dot{r}/c}$$

Here \dot{r} is the range rate or time derivative of the distance between the transmit antenna (ground) and satellite antenna at the time of reception, f_t is the ground transmit frequency, f_b is an offset frequency, f_s is the satellite spin rate (M/N) is the turnaround ratio of the satellite transponder, and s_r and s_t are the signs of the frequency shifts on reception and transmission which assume the values plus or minus one depending upon the direction of spin and the polarity of the receive and transmit antennas. In order to clarify what is meant here, consider Figure 1 which is redrawn from Reference 3. The model used for the turnstile antenna is a pair of crossed Hertzian dipoles which lies in the xy plane and rotates about the z-axis with a constant angular speed ω_s . Since the angular velocity vector, based on a right-hand rule, points along the positive z-axis, the rotation is counterclockwise when viewed from a point on the positive z-axis. If the antenna is being used to transmit and the polarization is right-hand circular* (as indicated in Figure 1), the sense of spin and polarization are the same and $s_t = +1$. If the polarization on transmit were left-hand circular and the angular velocity vector again pointed along the positive z-axis, $s_t = -1$. In

*The definition of right-hand circular polarization as standardized by the IRE is as follows: for an observer looking in the direction of propagation, the rotation of the electric-field vector in a transverse plane is clockwise for right-hand polarization. Similarly, the rotation is counterclockwise for left-hand polarization.

REPRODUCED
FROM REFERENCE 3

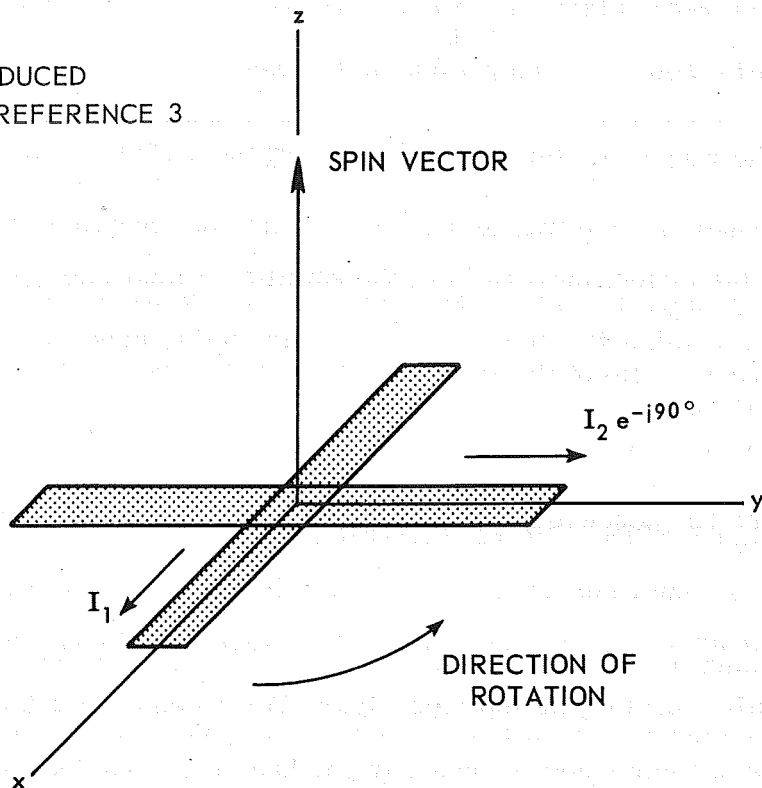


Figure 1. Turnstile Antenna Rotating in a Right-Handed Sense About the Positive z-axis, and Radiating a Right Hand Circularly Polarized Wave Along this Axis.

like manner, if the antenna is being used to receive and the polarization is right-hand, $s_r = +1$ (if left-hand, $s_r = -1$).

Solving (1) for \dot{r} we get approximately

$$\dot{r} = \frac{-c(f_o - f_b)}{2f_t + (f_o - f_b)} + \frac{(s_r + s_t)(M/N)}{2} \lambda_t f_s \quad (2)$$

Thus, the second term in (2) is an addition to the range rate measurement due to satellite spin. The magnitude of this term can be represented by

$$|\Delta \dot{r}| = \frac{|(1 \pm 1/k)|}{2} \lambda_t f_s \quad (3)$$

where k is the turn-around ratio of the satellite transponder, and $\lambda_t = c/f_t$ is the transmit wavelength. If $s_r = s_t$, the plus sign is used. If $s_r = -s_t$, the minus sign is used.

THE EXPECTED RANGE RATE BIAS DUE TO SATELLITE SPIN FOR EXPLORER 34

The orientation of Explorer 34 was such that its spin axis was perpendicular to the celestial equator, its top (see Figure 2) pointed toward the south celestial pole, and its angular velocity vector (right-hand rule) pointed toward the south celestial pole also; that is, if one looked at the top of the spacecraft from the direction of the south celestial pole, the spacecraft was spinning counterclockwise (Reference 5). During the time period covered in this analysis, the spin rate obtained from telemetry data was .38Hz (Reference 5). From Reference 1 (Appendix A) the polarity of the transmit antenna was left-hand circular off the top (as one looked toward the south celestial pole at the receding transmit wave, the tip of the electric vector rotated counterclockwise) and the polarity of the receive antenna was right-hand circular off the top. Therefore, from the previous discussion, $s_t = -1$, and $s_r = +1$. Since $(M/N) = 12/13$ for the Goddard Range and Range Rate System and $\lambda_t = 2.022$ meters for VHF satellites, the

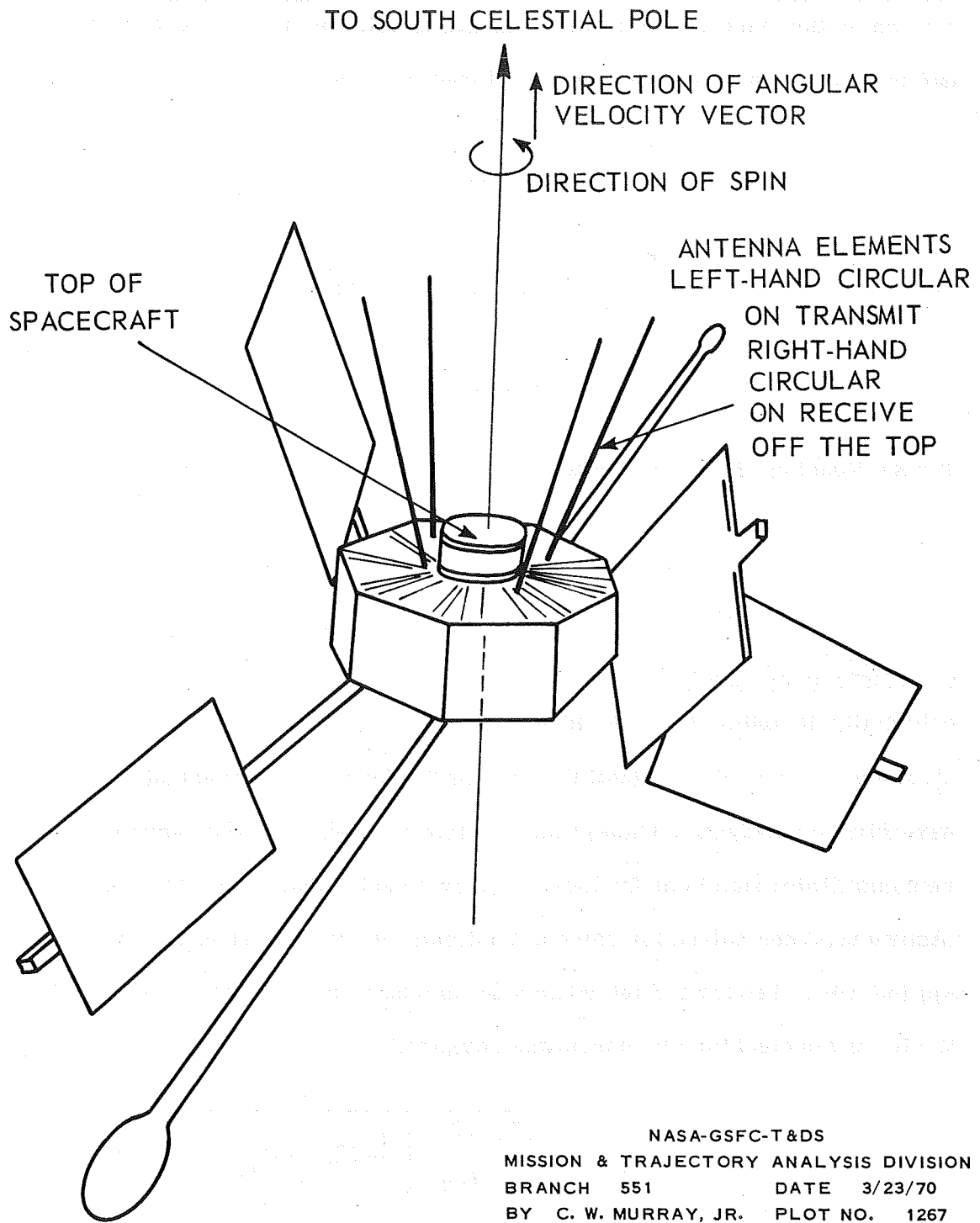


Figure 2. Geometrical Configuration of Explorer 34

addition to the range rate measurement due to spin (or the "correction" to be applied to the range rate data) is from Equation (2) above

$$\begin{aligned} \Delta \dot{r} &= \frac{(s_r + s_t / (M/N))}{2} \lambda_t f_s \\ &= \left[\frac{+1 - (1/(12/13))}{2} \right] (2.022) (.38) \\ &= -0.032 \text{ meters/second.} \end{aligned}$$

or from Equation (2) we can write

$$\begin{aligned} \dot{r}_{\text{measured}} &= \dot{r}_{\text{true}} + \text{bias} \\ &= \dot{r}_{\text{true}} + 0.032 \text{ meters/second} \end{aligned} \quad (4)$$

SOLUTION FOR RANGE RATE BIAS USING ORBIT DETERMINATION TECHNIQUES

Using an Orbit Determination Program (Reference 6) a constant range rate correction (correction = -bias) was effectively added to all the range rate measurements (Reference 7) of Explorer 34 over selected data arcs. The state of the satellite was then solved for using a Maximum Likelihood estimation procedure (Appendix B). The total weighted root mean square error over all observations for all stations and for all passes was computed

$$\sigma_{\text{Total}} = \sqrt{\frac{1}{n - (k + 1)} \sum_{i=1}^m \sum_{j=1}^{n_m} \left[\frac{1}{\sigma_i} (\hat{z}_{ij} - f_{ij}(x^*)) \right]^2} \quad (5)$$

where n_i is the number of observations of the i th data type, k is the number of parameters being estimated in the mathematical model, $n = n_1 + n_2 + \dots + n_m =$

total number of observations, m is the number of different data types, σ_i is the a priori standard deviation of the i th data type, and $\hat{z}_{ij} - f_{ij}(x^*)$ is the residual from the assumed model.

The above was done for three different epochs and the total weighted rms plotted as a function of the range rate bias in centimeters/second.* The results of the analysis can be seen in Figures 3, 4, and 5. In Figure 3 three different weighting schemes were used and in each case after fitting a least squares parabola to the rms values, a minimum of approximately 6 centimeters/second resulted. In Figure 4 after fitting a parabola to the rms values a minimum also occurred at approximately 6 centimeters/second. In Figure 5 using only range rate data in one case and using range and range rate data in the other case, after fitting with a parabola, a minimum occurred at approximately 2.5 centimeters/second.

From the previous paragraph approximately 3 centimeters/second bias can be accounted for due to the spin of the satellite. It is felt that the difference between the bias due to the spin and that "solved for" can be attributed to the effects of the ionosphere, since there were no ionospheric corrections made to the raw range rate data.

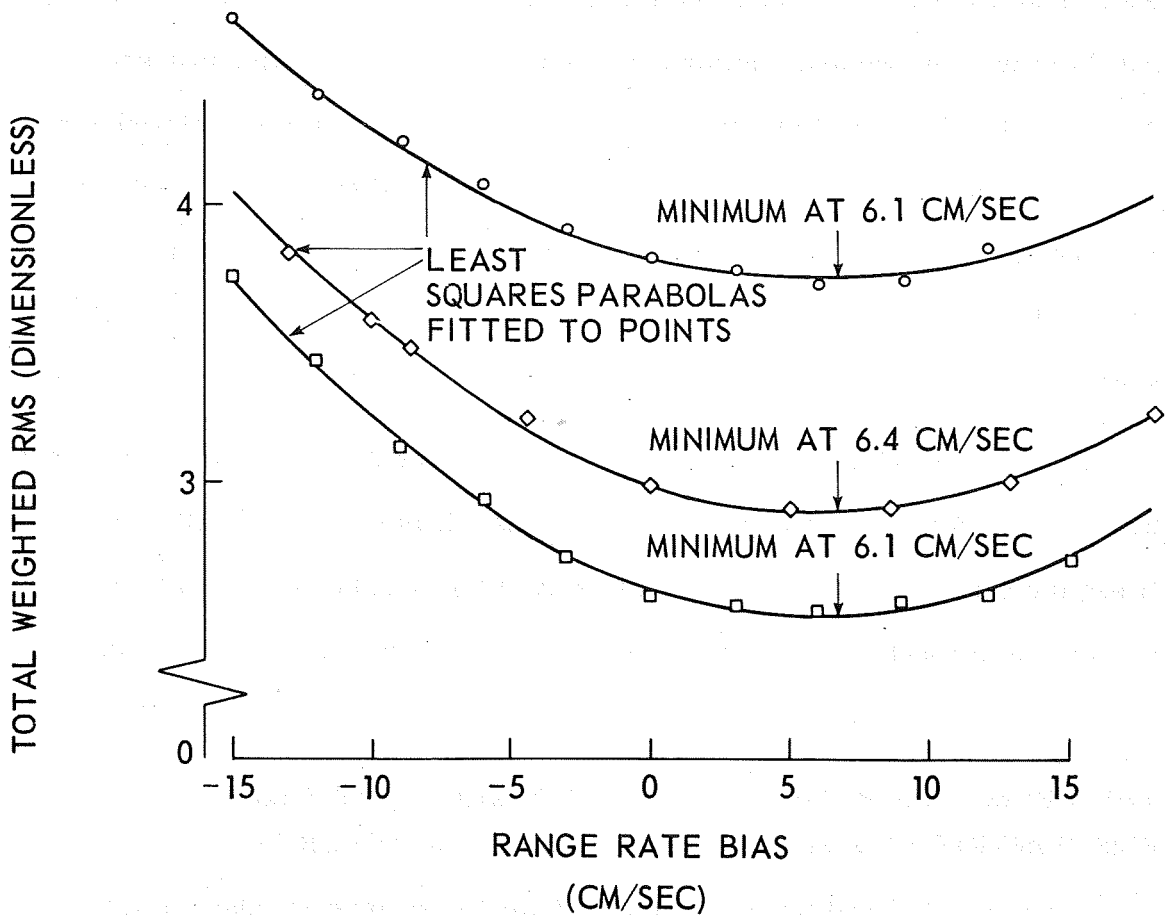
THE EFFECT OF RANGE RATE BIAS ON THE ORBIT AND RMS POSITION AND VELOCITY ERRORS OF EXPLORER 34

Using 925 Goddard Range and Range Rate Measurements taken on Explorer 34 from 26 August 1968 to 4 September 1968 (approximately two revolutions of the satellite) at Madagascar, Santiago, Carnarvon, and Rosman, the state vector was

* Adding a correction (correction = -bias) to all the range rate measurements is the same as adding the bias to the calculated values in the orbit determination program.

NOTE: 925 GRARR observations from 8/26/68 (19^h 42^m GMT) to 9/4/68 (3^h 41^m GMT) used to solve for state of Explorer 34 on above epoch (2 revolutions of satellite) with NONAME Orbit Determination Program

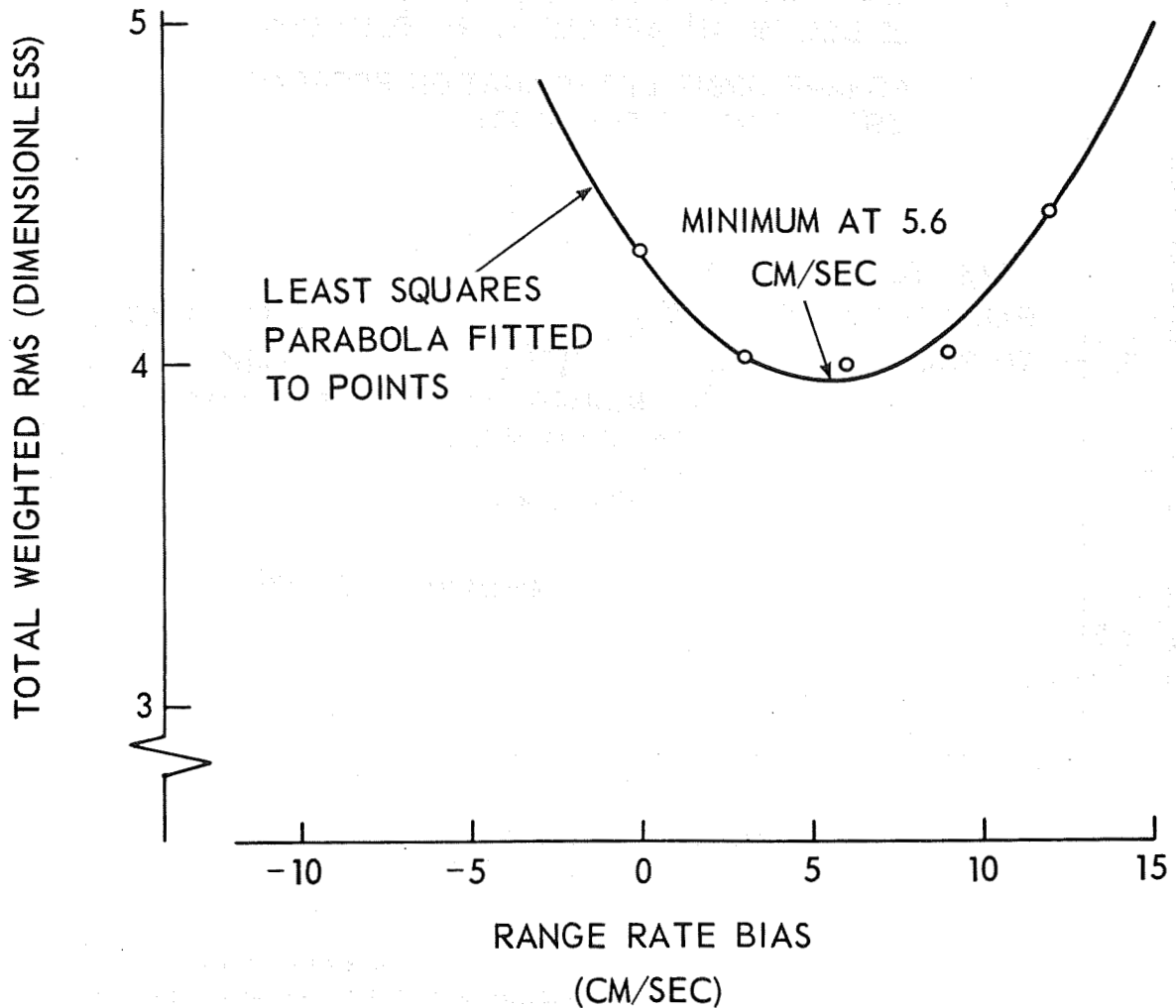
LEGEND	APRIORI WEIGHTING	
○	$\sigma_r = 100$ METERS	$\sigma_v = 5$ CM/SEC
◇	$\sigma_r = 150$ METERS	$\sigma_v = 5$ CM/SEC
□	$\sigma_r = 200$ METERS	$\sigma_v = 5$ CM/SEC



NASA-GSFC-T&DS
MISSION & TRAJECTORY ANALYSIS DIVISION
BRANCH 551 DATE 3/23/70
BY C. W. MURRAY, JR. PLOT NO. 1268

Figure 3. Total Weighted RMS vs Range Rate Bias – Explorer 34 Epoch, 26 August '68 13^h 55^m GMT

NOTE: 1461 GRARR observations from 30 Aug '68 (18^h 2^m GMT) to 13 Sept '68 (1^h 1^m GMT) used to solve for state of Explorer 34 on above epoch (3 revolutions of satellite) with NONAME Orbit Determination Program



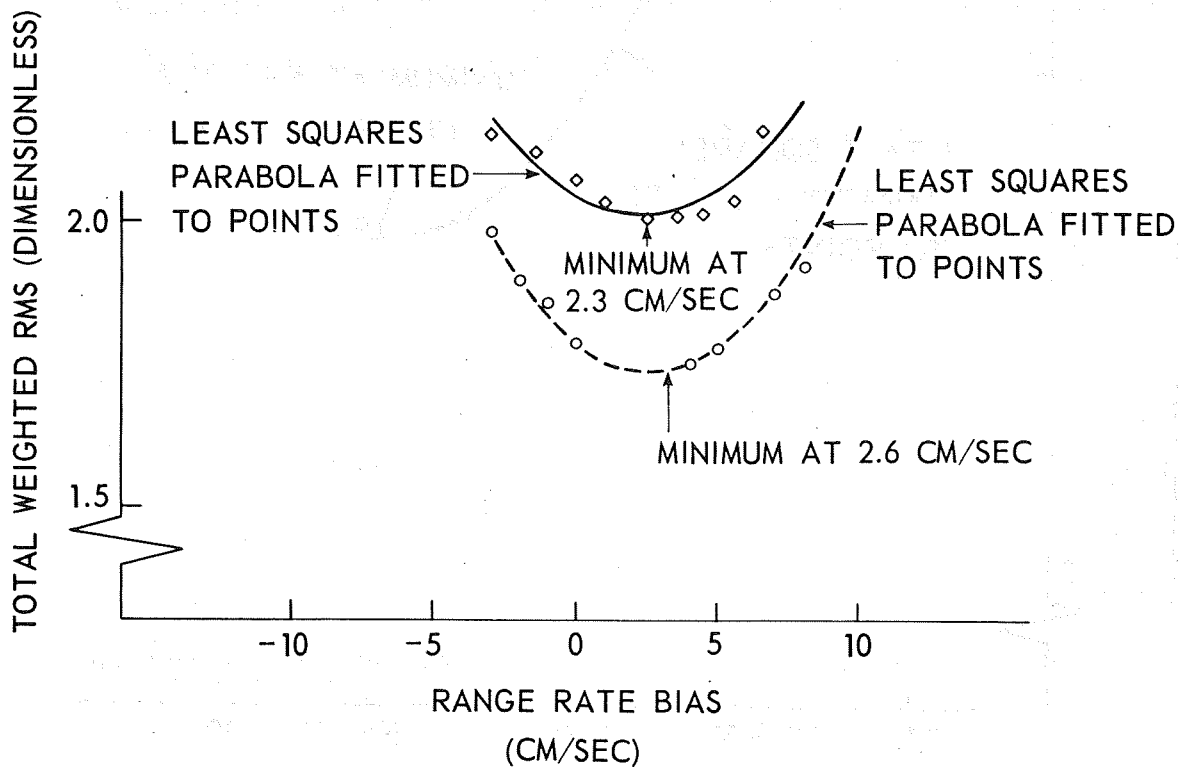
NASA-GSFC-T&DS
MISSION & TRAJECTORY ANALYSIS DIVISION
BRANCH 551 DATE 3/23/70
BY C. W. MURRAY, JR. PLOT NO. 1269

Figure 4. Total Weighted RMS vs Range Rate Bias – Explorer 34 Epoch, 30 August 1968 13^h 55^m GMT

LEGEND

- ◇ 810 GRARR OBSERVATIONS FROM 14 DEC '68 2^h 43^m GMT TO 22 DEC '68 17^h 42^m GMT (2 REVOLUTIONS)
- 364 i OBSERVATIONS FROM 14 DEC '68 9^h 9^m GMT TO 22 DEC '68 17^h 42^m GMT (2 REVOLUTIONS)

NONAME ORBIT DETERMINATION PROGRAM
USED TO SOLVE FOR STATE



NASA-GSFC-T&DS
MISSION & TRAJECTORY ANALYSIS DIVISION
BRANCH 551 DATE 3/23/70
BY C. W. MURRAY, JR. PLOT NO. 1270

Figure 5. Total Weighted RMS vs Range Rate Bias - Explorer 34 Epoch,
13 December 1968 15^h 21^m GMT

determined for the epoch 26 August 1968, 13 hours, 55 minutes GMT, by Reference 6. The solution can be seen in Table 1 where the coordinates are in a geocentric system (Appendix C).

A bias of +6 centimeters per second was added to all of the above range rate measurements and the state vector again determined using Reference 6. This was also done for a bias of -6 centimeters per second. The deviations of these "final" states from the "nominal" (no bias) determined above are also shown in Table 1. It can be seen that the difference in magnitude of the range at epoch is almost a kilometer while the difference in magnitude of the velocity at epoch is about 0.2 centimeters per second.

The state vector for each of the biased range rate measurements was propagated through the time period covering the data arcs and the position and velocity differences (referred to the above geocentric coordinate system) from the nominal state at five minute intervals — radial, cross track, and down track (see Appendix C) — calculated. An RMS for all the differences was calculated for the radial, cross track, and down track errors for both position and velocity. Finally, a total RSS position error and RSS velocity error was calculated. These can be seen in Table 1. The RSS position error is on the order of a half a kilometer while the RSS velocity error is on the order of 1 to 2 centimeters per second.

DISCUSSION

It should be noted that the bias in the range rate measurements (measurement = true value + bias) due to satellite spin is of one sign (in the case of Explorer 34 the sign is positive from Equation (4)). For the time period covered

Table 1

Effect of a Fixed Bias of +6 Centimeters/Second and -6 Centimeters/Second
in Range Rate Upon the Orbit of Explorer 34

State Vector* For Explorer 34 on 26 August 1968, 13h, 58m GMT

x (km)	y (km)	z (km)
-184543.28919	45942.39829	3895.13588
\dot{x} (m/s)	\dot{y} (m/s)	\dot{z} (m/s)
-654.99685	13.97573	451.67908

Deviation From Above State Vector When A Fixed 6 cm/sec Bias
Is Added To All Range Rate Observations

Δx (meters)	Δy (meters)	Δz (meters)	RSS
176	698	551	907
$\Delta \dot{x}$ (cm/sec)	$\Delta \dot{y}$ (cm/sec)	$\Delta \dot{z}$ (cm/sec)	
0.09	0.02	0.13	0.16

Deviation From Above State Vector When A Fixed -6 cm/sec Bias
Is Added To All Range Rate Observations

Δx (meters)	Δy (meters)	Δz (meters)	RSS
-177	-639	-451	802
$\Delta \dot{x}$ (cm/sec)	$\Delta \dot{y}$ (cm/sec)	$\Delta \dot{z}$ (cm/sec)	
-0.06	-0.04	-0.11	0.13

Root Mean Square of Radial, Cross, and Along Track Errors
For 8 Day Arc (From 8/27/68 to 9/5/68)

+6 cm/sec bias

	Radial	Cross Track	Down Track	RSS
Pos	64m	649m	246m	697m
Vel	1.44cm/s	.78cm/s	.22cm/s	1.65cm/s

-6 cm/sec bias

Pos	11m	587m	196m	619m
Vel	.18cm/s	.69cm/s	.17cm/s	.73cm/s

*Referred to the following geocentric coordinate system. The fundamental plane is the true equator of the epoch, x axis directed towards the true vernal equinox of the epoch, z axis perpendicular to the fundamental plane with the positive z direction north, y axis perpendicular to x and z so as to form a right-handed Cartesian Coordinate System.

in this analysis the spin rate was for all practical purposes constant (.38 Hz). Therefore, by adding a "correction" of the opposite sign to all the range rate measurements and then solving for the state vector at epoch, the total weighted rms of fit (Equation (5)) will be reduced. Since there were no ionospheric corrections applied to the range rate data it is felt that the difference between the bias as predicted due to spin and that as "solved for" (Figures 3, 4, and 5) can be attributed to the effect of the ionosphere.

From Reference 8 the contribution to the phase of the two-way Doppler signal $\Delta\phi_R(t)$, due to the effect of the ionosphere (neglecting the magnetic field) is given by (from Equation 32 of Reference 8)

$$\Delta\phi_R(t) = \frac{2\omega_t I}{c f_{eq}^2} \quad (6)$$

where the quantities in the above equation are given by

$$\frac{1}{f_{eq}^2} = \frac{1}{2} \left\{ \frac{1}{f_t^2} + \frac{1}{f_d^2} \right\}$$

f_t = transmit or uplink frequency

ω_t = $2\pi f_t$ = uplink angular frequency

f_d = downlink frequency

c = speed of light

and I , proportional to the total electron count, is given by

$$I = \int_0^R \mu ds$$

where R is the range,

$$\mu = \frac{4\pi N_e \epsilon^2}{m(2\pi)^2}$$

N_e = electron density in electrons/cm³

ϵ = the electron charge (4.8×10^{-10} esu)

m = electron mass (9.1×10^{-28} gm)

Differentiating (6) and converting to range rate, we obtain an addition (bias) to the true range rate due to the ionosphere

$$\Delta \dot{r}_I = - \left(\frac{1}{f_{eq}^2} \right) \frac{dI}{dt} \quad (7)$$

For short data arcs we can consider I a function of elevation angle E only.

Therefore

$$\Delta \dot{r}_I = - \left(\frac{1}{f_{eq}^2} \right) \left(\frac{dI}{dE} \right) \left(\frac{dE}{dt} \right) \quad (8)$$

From Equation (8) we see that the effect of the ionosphere on range rate will be positive or negative, depending upon the sign of dE/dt .

It should be noted that the range rate bias being discussed here is different from that due to the bending of the electromagnetic waves at the vehicle. This latter effect results from the local index of refraction and is more pronounced within the ionosphere. Above the ionosphere (above 1000 kilometers) the angle between the line of sight path and the signal path is reduced and therefore the bias due to this effect is reduced. The range rate bias indicated in (8) is frequency dependent. Since the ionosphere is a dispersive medium the velocity of

propagation varies as a function of frequency, and approaches vacuum velocity as the frequency increases. In order to assess the effect of the ionosphere upon range rate at VHF we will assume for the moment a simple model for the ionosphere which is plane-stratified with only vertical gradients

$$I = \frac{40.3 I_v}{\sin E} \quad (9)$$

where I_v is the total electron content along the vertical.

In order to obtain an idea of the magnitude of $\Delta \dot{r}_I$ in (8) for VHF, let $f_d = 136$ MHz (Explorer 34) and $f_t = 148.26$ MHz (GRARR VHF transmit frequency). Letting $E = 60^\circ$, and using a value for I_v of 10^{17} electrons/meter (Reference 9), for an elevation angle rate of 25×10^{-5} radians/second, from (8) and (9) we have

$$\begin{aligned} \Delta \dot{r}_I &= \frac{1}{f_{eq}^2} \left\{ \frac{(40.3) \cos E}{\sin^2 E} \right\} \left(\frac{dE}{dt} \right) I_v \\ &= 0.03 \text{ meters/second} \end{aligned} \quad (10)$$

Considering the magnitude and the sign of the bias due to the ionosphere, it can be seen that the net effect for all stations and all passes over 2 to 3 revolutions of the satellite in its orbit could be positive or negative and on the order of a few centimeters per second since the biases from certain passes would tend to cancel the biases from other stations and passes. For this reason and also since there were no corrections made for the ionosphere within the program, it is felt that the difference between the bias as predicted due to the spin and the bias as "solved for" is due to the ionosphere. This will be investigated

more thoroughly. It is still felt, however, that the results of this analysis as shown in Figures 3, 4, and 5, substantiate the effect of satellite spin on the range rate measurements and verify the theoretical predictions in Reference 3.

A similar type analysis is being conducted for Explorer 35 which is in lunar orbit.

In addition to the above analysis the spin bias has been experimentally verified in tests conducted at Rosman which simulated a rotating satellite antenna at S-Band using an S-Band pole beacon, the S-Band tracking system, and a rotating conical spiral antenna (Reference 10).

CONCLUSIONS

The results of this analysis may be summarized in the following.

- (1) A bias of several centimeters per second in the two-way Doppler range rate measurements of Explorer 34 has been detected through orbit determination techniques. Approximately 3 centimeters per second bias in the range rate measurements is due to the effect of satellite spin (Reference 3).
- (2) The rms of fit was reduced when a "correction" of opposite sign to the predicted bias due to spin was added to all the range rate measurements and the state vector of Explorer 34 at epoch "solved for" using orbit determination techniques. In this sense the predicted bias has been verified.

ACKNOWLEDGMENTS

The author wishes to thank C. E. Doll, Jr., Code 552, for showing him how to run the NONAME program and how to effectively add a constant bias to the range rate measurements through the program and Eugene Lefferts of the Mission and Trajectory Analysis Division (Code 551) for many discussions on the Maximum Likelihood Estimator for non-linear models, in particular, his proof that the estimator is unbiased under the assumption of linearity. In addition the author wishes to thank Mr. Paul E. Schmid, Jr. for many helpful discussions on the effects of the ionosphere on the range rate measurements.

REFERENCES

1. Jackson, R. B., "The Canted Turnstile As An Omni-Directional Spacecraft Antenna System", NASA (GSFC), X-712-67-441, September '67.
2. Marini, J. W., and Murray, C. W., Jr., "Effect of Satellite Spin On Explorer 33 and 35 Doppler Tracking Data", NASA (GSFC), X-551-69-52, February 1969.
3. Marini, J. W., "The Effect Of Satellite Spin On Two-Way Doppler Range-Rate Measurements", NASA (GSFC), X-551-69-104, March 1969.
4. Kruger, B., "The Doppler Equation In Range and Range Rate Measurements", NASA (GSFC), October 1965.
5. Limberis, W. L., Private Communication.

6. NONAME, An Orbit and Geodetic Parameter Estimation System, prepared by Wolf Research and Development Corporation for Mission and Trajectory Analysis Division, NASA (GSFC).
7. Doll, Jr., C. E., Private Communication.
8. Memo from H. C. Parker, RCA to J. H. Berbert, Head Operations Evaluation Branch on GRARR Ionospheric Errors, 28 November 1969.
9. Rosenbaum, B., "Ionospheric Perturbations On Stadan VHF Tracking Accuracy", NASA (GSFC), X-551-69-403, September 1969.
10. Marini, J. W., "A Test of the Effect of Satellite Spin on Two-Way Doppler Range-Rate Measurements," NASA/GSFC Document to be published shortly.
11. Anderson, John D., "Theory of Orbit Determination - Part II, Estimation Formulas", Technical Report No. 32-498, Jet Propulsion Laboratory, October 1, 1963.
12. Kendall, M. G., and Stuart, A., "The Advanced Theory of Statistics", Volume 2, Hafner Publishing Company, N.Y. (1967), Chapters 17, 18, and 19.

APPENDIX A

THE ANTENNA CONNECTIONS ON EXPLORER 34

Figure A-1 shows both a top and side view of Explorer 34 which made use of a canted turnstile antenna (Reference 1) consisting of four quarter wave monopoles symmetrically located about the axis of spin of the satellite. The geometrical configuration of the elements can be seen as one looks down on the "top" of the satellite.

Figure A-2 shows the feed system or electrical configuration of the antenna elements which were fed with relative phase angles of 0° , 90° , 180° , and 270° so that opposing terminals were 180° out of phase.

In order to determine the polarization of the transmit and receive antennas (from A-2 it can be seen that the same antenna elements are used for transmit and receive, the transmit frequency being 136 MHz and the receive frequency 148 MHz) from these two figures consider first the transmit case. In A-2, tracing the electrical signal from the output of the Diplexer at point A, the phase of the current at Antenna #1 leads the phase of the current at Antenna #2 by 90° , and the phase of the current at Antenna #4 lags by 180° the phase at Antenna #2, while the phase at Antenna #3 lags by 180° the phase at Antenna #1. Thus, still retaining the relative physical configuration of the antenna elements as shown in A-1 and looking down on the "top" of the spacecraft (that is, towards the north celestial pole since the "top" faces the south celestial pole), at some time t_0 , the relative phases of the elements will be as indicated in Figure A-3.

Since a center-fed dipole is equivalent to two opposing monopoles fed 180° out of phase to each other, A-3 can be represented in a different way. Thus,

REPRODUCED
FROM REFERENCE 1

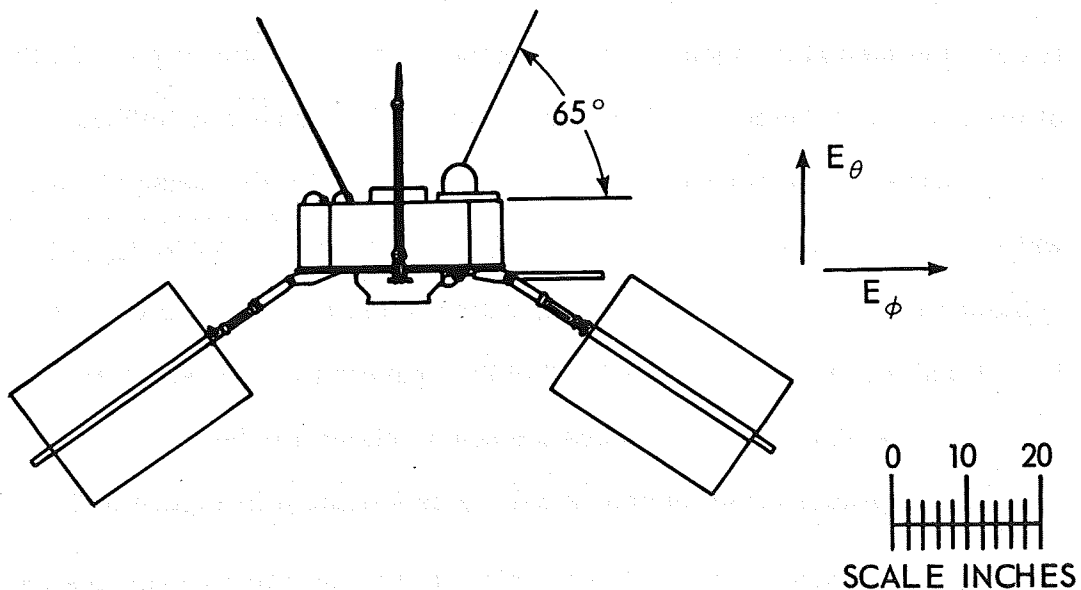
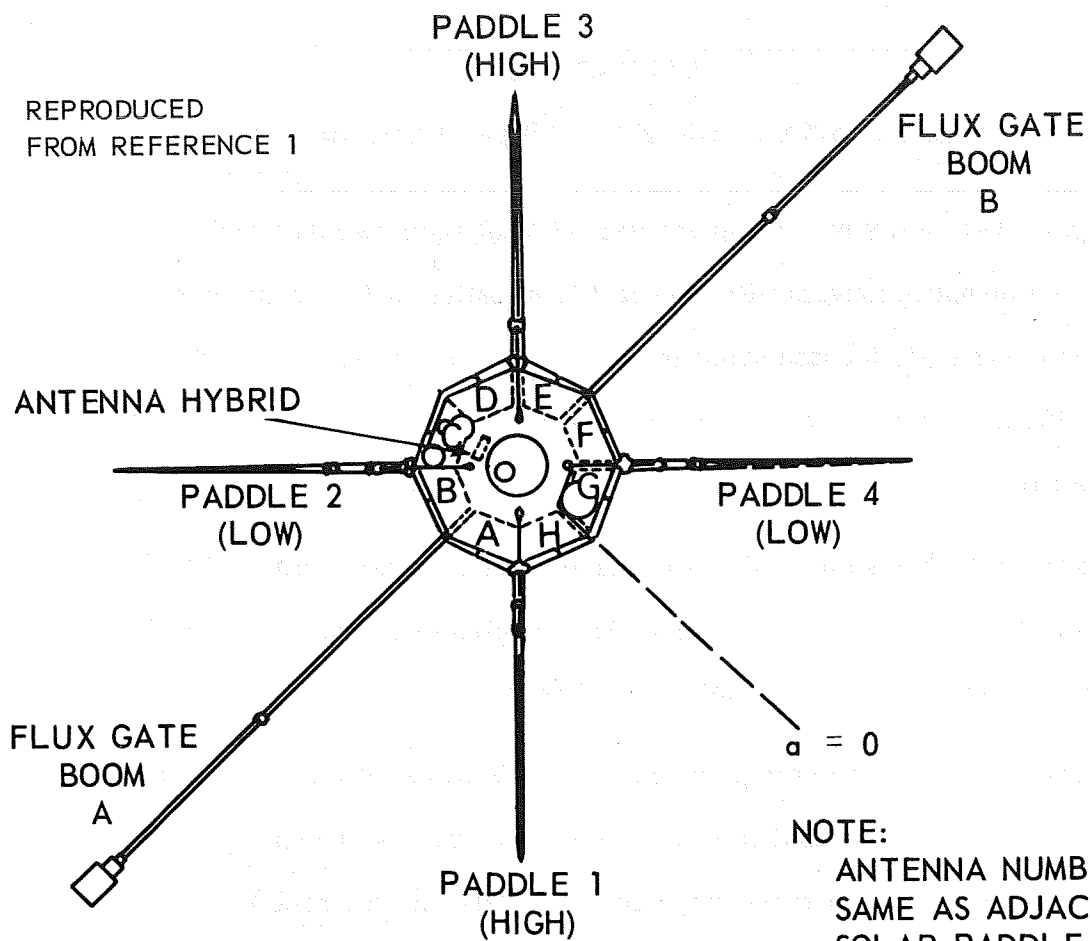
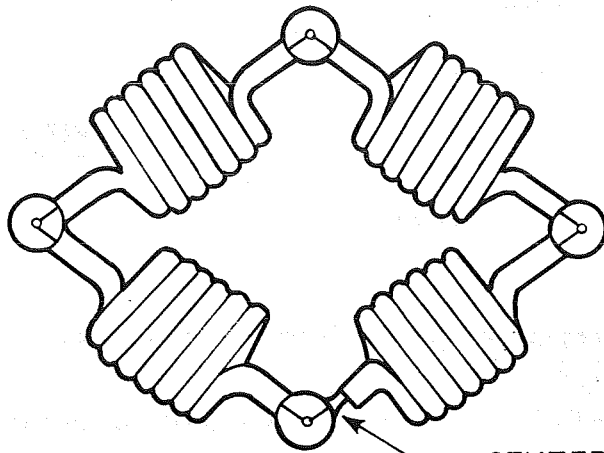


Figure A-1. Explorer 34 Satellite



REPRODUCED
FROM REFERENCE 1

CENTER CONDUCTOR REVERSED

ALL CABLES $70\ \Omega$ COAX
LENGTH = $\lambda/4$ AT CENTER FREQUENCY

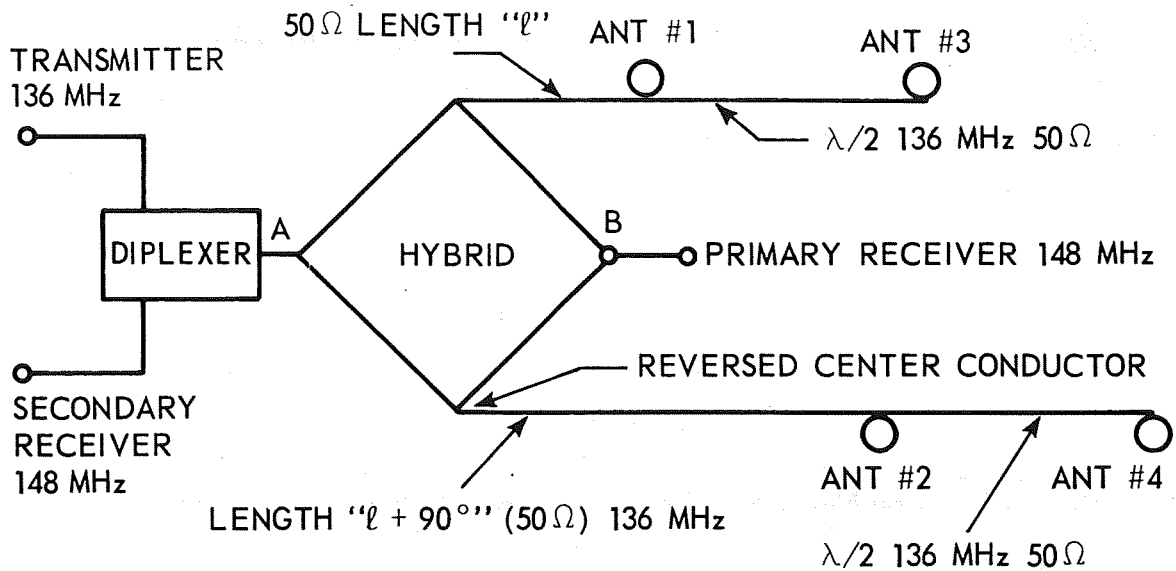


Figure A-2. Explorer 34 Feed System

transmit wave rotates in a counterclockwise direction, the polarization is left-hand circular.*

In the case of the receive antenna, we can consider the receiver at B to be a transmitter (reciprocity theorem for antennas). Then, at some time, say t_0 , the current flow will be as shown in A-6 (again looking down at the "top" and using the dipole representation)

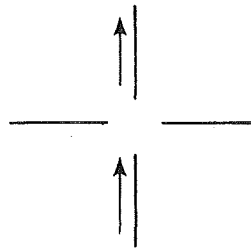


Figure A-6. Current Flow at Some Reference Time t_0 (Receive) Under Dipole Representation

and later as indicated in A-7.

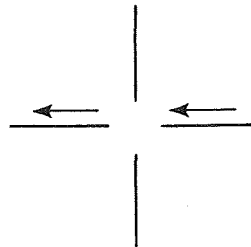


Figure A-7. Current Flow at Some Later Time (Receive) Under Dipole Representation

Note that from Figure A-2, the reversed center conductor shifts the phase by 180° . Thus, considering the receiver as a transmitter, as one looks at the receding transmit wave (in the direction of the south celestial pole), the electric vector rotates clockwise. Therefore, the polarization is right-hand circular "off the top" on receive.

*For an observer looking in the direction of propagation, the rotation of the electric-field vector is clockwise for right-hand circular polarization. Similarly, the rotation is counter clockwise for left-hand circular polarization (standard IRE definition).

APPENDIX B

MAXIMUM LIKELIHOOD ESTIMATION IN THE ORBIT DETERMINATION PROCESS

A somewhat similar type discussion of the Maximum Likelihood Estimation may be found in Reference 11.

In orbit determination what we are generally presented with is the following. A large number of measurements (range, range rate, angle data, for example) is available. In contrast, the orbit of the spacecraft is defined by a relatively small number of parameters (the initial state vector of the spacecraft in the Newtonian equations of motion plus physical constants which appear in the mathematical description of that motion, for example). Therefore, in practice, the system is overdetermined. A logical question to ask at this point is, "Assuming that a reasonably adequate mathematical model exists for the data, what is a 'best' estimate for the parameter set defining the model?" In order to answer this question, however, a definition of "best" has to be made. If we consider that to each measurement there can be associated some random type error, and further, that to this random error a probability distribution can be described, we will then be in a position to define what we mean by "best" in a statistical or probability sense.

In the following discussion we will develop a rationale or motivation underlying the use of Maximum Likelihood Estimation in the Orbit Determination Process. By the term "best" we will mean that estimate of the parameter set which maximizes the joint probability of occurrence of the given measurement set and an a priori parameter set. In other words, what we are saying is that by

the Method of Maximum Likelihood, it is assumed that the combined a priori parameter set and the observed data set is the one most likely to occur. It will be seen further that under the assumptions given below, the estimator in the Maximum Likelihood Method is the same as the estimator in the Least Squares Method, is unbiased, has minimum variance, and is sufficient. The assumption of normality is required to equate the two methods. The assumption of linearity "in the neighborhood" of the solution is necessary to show unbiasedness, minimum variance and sufficiency.

Let \hat{z} be an $(n \times 1)$ measurement vector and $f(x)$ a nonlinear model which it is assumed adequately describes the measurements, where x is a $(k \times 1)$ parameter vector. Since to each measurement there will be associated some error, we can write

$$\hat{z} = f(x) + \eta \quad (B-1)$$

where η is an $(n \times 1)$ error vector.

Let η be a random vector (multidimensional random variable) representing the measurement error such that

$$\begin{aligned} \bar{E}(\eta) &= 0 \\ \text{Var}(\eta) &= A_z \end{aligned} \quad (B-2)$$

Then we can write

$$\hat{Z} = f(X) + \eta \quad (B-3)$$

where X and \hat{Z} are also random vectors (functions of random variables are random variables) each of which has a unique probability distribution. Let $p(x)$

be the probability density for X and $p(\hat{z})$ the probability density for \hat{Z} . Then the joint probability density $p(x, \hat{z})$ of X and \hat{Z} can be written in terms of conditional densities

$$p(x, \hat{z}) = p(x) p(\hat{z}/x) = p(\hat{z}) p(x/\hat{z})$$

or

(B-4)

$$p(x/\hat{z}) = \frac{p(x)}{p(\hat{z})} p(\hat{z}/x)$$

where $p(x/\hat{z})$ is the conditional probability that X occurs given that \hat{Z} has occurred and $p(\hat{z}/x)$ is the conditional probability that \hat{Z} occurs given that X has occurred. The second expression in (B-4) is Bayes Theorem relating conditional probabilities.

From (B-4) if $p(x)$ and $p(\hat{z}/x)$ are known, then $p(x, \hat{z})$ can be evaluated as a function of x , and hence, the probability of the joint occurrence of X and \hat{Z} will be known. It seems reasonable, therefore, to select as an estimator X^* for x , one that maximizes this joint probability density function. To determine this estimator, however, the form of the probability density function must be known (unlike the method of Least Squares where no such probability distribution assumption need be made). We will assume that both X and \hat{Z} given X have a multivariate normal distribution with the following expressions

$$p(x) = k_x \exp \left(-\frac{1}{2} (x - \bar{x})^T A_x^{-1} (x - \bar{x}) \right)$$

$$p(\hat{z}/x) = k_z \exp \left(-\frac{1}{2} (\hat{z} - f(x))^T A_z^{-1} (\hat{z} - f(x)) \right) \quad (B-5)$$

$$-\infty < x_i < \infty$$

$$-\infty < f_j < \infty$$

where $k_x = (2\pi)^{-k/2} |A_x|^{-1/2}$, $k_z = (2\pi)^{-n/2} |A_z|^{-1/2}$, $i = 1, 2, \dots, k$, $j = 1, 2, \dots, n$, A_x is the covariance matrix for X , \hat{x} is the mean value of X , A_z is the covariance matrix for \hat{Z} given X , and $f(x)$ is the mean value of \hat{Z} given X .

Under the assumption of a normal distribution for X , the vector \hat{x} is the most likely description of the orbit without the inclusion of the measurement vector \hat{z} , and A_x represents the confidence that we have in \hat{x} . For this reason, \hat{x} is called the apriori parameter set and A_x the apriori covariance matrix. It doesn't seem unreasonable to assume a normal distribution for X in the sense that if the launch vehicle, for instance, has been designed properly (its guidance and navigation instrumentation), there will be a preflight or nominal parameter set defining the orbit which has the greatest likelihood of occurring. Other values for the parameter set would have a smaller chance of occurring (for instance an orbit going through the earth). We can therefore intuitively rationalize the assumption of normality for X . With respect to the vector \hat{x} , in many cases, it will represent a preflight nominal or design vector and A_x a matrix which has been "built up" from a number of error sources within the guidance and control system of the launch vehicle. In other cases, \hat{x} might be a state vector which has been propagated in time through the equations of motion or an estimate of the state determined from another independent source with A_x being its associated covariance matrix.

With regard to the assumption of a normal distribution for \hat{Z} given X , we see from Equation (B-3) that if X is normally distributed, certainly a nonlinear function of X , $f(X)$, cannot be normally distributed (a normally distributed random variable can be written as a linear combination of normally distributed random

variables). Therefore, by assuming that \hat{Z} given X has a normal distribution, we are actually stating that η has a normal distribution and also that $f(x)$ can be expanded in a Taylor series about \hat{x} and the second order terms neglected.

$$f(x) \doteq f(\hat{x}) + \left. \frac{\partial f}{\partial x} \right|_{x=\hat{x}} (x - \hat{x}) \quad (\text{B-6})$$

Or, expressed somewhat differently, by assuming that \hat{Z} given X is normal (along with the assumption that X is normal), we are saying that η is normally distributed. That is, the method of measurement gives rise to errors which have a normal distribution.

The matrix A_z defined above is usually taken to be diagonal mainly for the purpose of ease in machine computation, since it will be seen later that this matrix has to be inverted. Thus, A_z will reflect the noise variances on the data types and can be obtained from a knowledge of system errors (equipment) or previous data analyses.

Let us now form the Likelihood Function L which is the joint probability of obtaining X and \hat{Z} .

$$L = k_x k_z \exp \left[-\frac{1}{2} (x - \hat{x})^T A_x^{-1} (x - \hat{x}) - \frac{1}{2} (\hat{z} - f(x))^T A_z^{-1} (\hat{z} - f(x)) \right] \quad (\text{B-7})$$

or since $(x - \hat{x})^T A_x^{-1} (x - \hat{x}) = (\hat{x} - x)^T A_x^{-1} (\hat{x} - x)$,

$$L = k_x k_z \exp \left[-\frac{1}{2} (\hat{x} - x)^T A_x^{-1} (\hat{x} - x) - \frac{1}{2} (\hat{z} - f(x))^T A_z^{-1} (\hat{z} - f(x)) \right] \quad (\text{B-8})$$

or in expanded form

$$L = k_x k_z \exp \left[-\frac{1}{2} w^T D^{-1} w \right] \quad (\text{B-9})$$

where

$$w = \begin{bmatrix} \tilde{x} - x \\ \hat{z} - f(x) \end{bmatrix}, \quad D = \begin{bmatrix} A_x & 0 \\ 0 & A_z \end{bmatrix}, \quad \xi \begin{bmatrix} \tilde{X} \\ \hat{Z} \end{bmatrix} = \begin{bmatrix} x \\ f(x) \end{bmatrix} \quad (\text{B-10})$$

Writing the Likelihood Function in the form (B-8) we can consider the apriori values as random variables or additional observations having mean x , that is, $\xi(\tilde{X}) = x$. Therefore, when we choose an estimate or a value x^* for x which maximizes L ,⁽¹⁾ this is the same as saying that the combined set of apriori values and the observed data was the one most likely to occur. Writing L in the form (B-9) we see that the joint density function for \tilde{X} and \hat{Z} is multivariate normal, that X and \hat{Z} given X are uncorrelated and therefore independent since they both have Gaussian distributions. It should be noted, however, that regardless of the form of the probability distributions for X and \hat{Z} given X , these two random variables will, by definition, be independent, since the joint distribution of X and \hat{Z} given X is the product of the density of X times the density of \hat{Z} given X .

The Likelihood Equation is obtained by taking the gradient of the logarithm of L and equating it to zero ($\log L$ attains its maximum for the same value of x as L)⁽²⁾

⁽¹⁾A distinction is made between the method of rule of estimation which we shall call an estimator and the value to which it gives rise in particular cases, the estimate. The distinction is the same as that between a function $f(x)$, regarded as defined for a range of the variable x , and the particular value which the function assumes, say $f(a)$, for a specified value of x equal to a (reference (11)).

⁽²⁾ L and $\log L$ have maxima together, since $\frac{\partial}{\partial x} \log L = L'/L$ and $L > 0$.

$$\log L = \log k_x k_z - \frac{1}{2} Q \quad (\text{B-11})$$

where Q is the quadratic form

$$Q = (\mathbf{x} - \hat{\mathbf{x}})^T \mathbf{A}_x^{-1} (\mathbf{x} - \hat{\mathbf{x}}) + (\hat{\mathbf{z}} - \mathbf{f}(\mathbf{x}))^T \mathbf{A}_z^{-1} (\hat{\mathbf{z}} - \mathbf{f}(\mathbf{x})) \quad (\text{B-12})$$

From (B-7) and (B-11) it can be seen that maximizing $\log L$ is equivalent to minimizing Q . Taking the gradient of $\log L$ with respect to \mathbf{x}

$$\mathbf{F}(\mathbf{x}) = \nabla_{\mathbf{x}} Q = \mathbf{B}^T \mathbf{A}_z^{-1} (\hat{\mathbf{z}} - \mathbf{f}(\mathbf{x})) + \mathbf{A}_x^{-1} (\hat{\mathbf{x}} - \mathbf{x}) \quad (\text{B-13})$$

where

$$\mathbf{B} = (b_{ij}) = \frac{\partial f_i(\mathbf{x})}{\partial x_j} = \mathbf{B}(\mathbf{x})$$

is an $(n \times k)$ matrix of rank $k < n$.

By neglecting the dependence of \mathbf{B} on \mathbf{x} , we can use a modified Newton-Raphson Iteration Technique to find a solution \mathbf{x}^* such that $\mathbf{F}(\mathbf{x}^*) = 0$ (other iteration schemes could certainly be used if they converge to a solution). Taking the gradient of (B-13)

$$\mathbf{F}'(\mathbf{x}) = \nabla_{\mathbf{x}}^2 Q = -\mathbf{B}^T \mathbf{A}_z^{-1} \mathbf{B} - \mathbf{A}_x^{-1} \quad (\text{B-14})$$

Since \mathbf{A}_x and \mathbf{A}_z are covariance matrices of multivariate normal distributions, they are by definition positive definite. \mathbf{A}_x^{-1} and \mathbf{A}_z^{-1} are therefore positive definite. Since \mathbf{B} was assumed to have rank $k < n$, $\mathbf{B}^T \mathbf{A}_z^{-1} \mathbf{B}$ is positive definite and also $(\mathbf{B}^T \mathbf{A}_z^{-1} \mathbf{B} + \mathbf{A}_x^{-1})$. Hence, the $(k \times k)$ matrix in (B-14) is negative definite, and if the process converges to \mathbf{x}^* , Q will be minimized and $\log L$ (therefore L) maximized.

In order to solve for x^* , denote by $x^{(m)}$ the estimate of the solution at the m^{th} iteration; then, the improved estimate of the solution $x^{(m+1)} = x^*$, using the Newton-Raphson formula will be (using B-13 and B-14)

$$\begin{aligned} x^* &= x^{(m+1)} = x^{(m)} - \left(\frac{F(x^{(m)})}{F'(x^{(m)})} \right) = x^{(m)} - \left(F'(x^{(m)}) \right)^{-1} F(x^{(m)}) \\ &= x^{(m)} + (B^T A_z^{-1} B + A_x^{-1})^{-1} \left\{ B^T A_z^{-1} (\hat{z} - f(x^{(m)})) + A_x^{-1} (\hat{x} - x^{(m)}) \right\} \end{aligned} \quad (\text{B-15})$$

where

$$B = B(x^{(m)}).$$

We will not prove some properties of the estimator X^* .

UNBIASED

df: An estimator X^* is said to be an unbiased estimator of x if $E(X^*) = x$.

From (B-13) when $x = x^*$

$$F(x^*) = B^T A_z^{-1} (\hat{z} - f(x^*)) + A_x^{-1} (\hat{x} - x^*) = 0 \quad (\text{B-16})$$

Expanding (B-1) in a Taylor series about $x = x^*$ and substituting in (B-16) gives

$$\begin{aligned} B^T A_z^{-1} \left\{ f(x^*) + B(x - x^*) + \eta + \text{higher order terms} - f(x^*) \right\} \\ + A_x^{-1} (\hat{x} - x) + A_x^{-1} (x - x^*) = 0 \end{aligned}$$

Neglecting the higher order terms and using random vector notation, then taking expectations

$$\left\{ B^T A_z^{-1} B + A_x^{-1} \right\} \xi[x - X^*] + A_x^{-1} \xi[\tilde{X} - x] + \xi(\eta) = 0$$

or

$$\xi(X^*) = x \quad (B-18)$$

and therefore X^* is an unbiased estimator of x .

MINIMUM VARIANCE

The fundamental inequality for the variance of an unbiased estimator t of x is the Cramér-Rao inequality

$$\text{Var } t \geq \frac{-1}{\xi\left(\frac{\partial^2 \log L}{\partial x^2}\right)} \quad (B-19)$$

The right-hand side of (B-19) is called the Minimum Variance Bound (MVB) for the estimator of x . An estimator which attains this bound for all x will be called a MVB estimator.

The necessary and sufficient condition that an unbiased estimator t be a MVB estimator of x is that the following holds

$$\frac{\partial \log L}{\partial x} = G(x) (t - x) \quad (B-20)$$

where G is independent of the observations but may be a function of x . If (B-20) is satisfied, then t is a MVB estimator of x with variance $1/G(x)$ which is equal to the right-hand side of (B-19).

In order for (B-19) to hold, L must be twice differentiable. But from (B-9), L is Gaussian and therefore exponential. Hence it is infinitely differentiable.

From (B-13) we have

$$\frac{\partial \log L}{\partial \mathbf{x}} = \mathbf{B}^T \mathbf{A}_z^{-1} (\hat{\mathbf{z}} - f(\mathbf{x})) + \mathbf{A}_x^{-1} (\hat{\mathbf{x}} - \mathbf{x}) \quad (\text{B-21})$$

When $\mathbf{x} = \mathbf{x}^*$, the solution, (B-21) is zero.

$$\mathbf{B}^T \mathbf{A}_z^{-1} (\hat{\mathbf{z}} - f(\mathbf{x}^*)) + \mathbf{A}_x^{-1} (\hat{\mathbf{x}} - \mathbf{x}^*) = 0 \quad (\text{B-22})$$

Solving for $\mathbf{B}^T \mathbf{A}_z^{-1} \hat{\mathbf{z}}$ in (B-22) and substituting it in (B-21) we have

$$\frac{\partial \log L}{\partial \mathbf{x}} = \mathbf{B}^T \mathbf{A}_z^{-1} (f(\mathbf{x}^*) - f(\mathbf{x})) + \mathbf{A}_x^{-1} (\mathbf{x}^* - \mathbf{x}) \quad (\text{B-23})$$

Expanding $f(\mathbf{x})$ in a Taylor series about the solution $\mathbf{x} = \mathbf{x}^*$, neglecting second order terms and higher, (B-23) becomes

$$\frac{\partial \log L}{\partial \mathbf{x}} = (\mathbf{B}^T \mathbf{A}_z^{-1} \mathbf{B} + \mathbf{A}_x^{-1}) (\mathbf{x}^* - \mathbf{x}) \quad (\text{B-24})$$

where

$$\mathbf{B} = \mathbf{B}(\mathbf{x}^{(m)}).$$

Comparing (B-24) with (B-20) we see that \mathbf{X}^* is a MVB estimator of \mathbf{x} with variance

$$1/G = (\mathbf{B}^T \mathbf{A}_z^{-1} \mathbf{B} + \mathbf{A}_x^{-1})^{-1} \quad (\text{B-25})$$

It should be noted that the property of minimum variance for \mathbf{X}^* depended upon expanding $f(\mathbf{x})$ in a Taylor series about \mathbf{x}^* and neglecting second order terms and higher. Thus, within the region of linearity, \mathbf{X}^* is a minimum variance estimator of \mathbf{x} .

To determine the Cramér-Rao Lower Bound, taking the second gradient of $\log L$ with respect to x (Equation (B-14)) we have

$$\frac{\partial^2 \log L}{\partial x^2} = -B^T A_z^{-1} B - A_x^{-1} \quad (B-26)$$

where B is independent of x . Since (B-26) is a constant, taking the expectation of this quantity leaves it unchanged. Therefore, (B-19) becomes

$$\text{Var } t \geq (B^T A_z^{-1} B + A_x^{-1})^{-1} \quad (B-27)$$

SUFFICIENCY

df: if the Likelihood Function L can be written as

$$L = g(x^*/x) k(\tilde{x}, \hat{z}) \quad (B-28)$$

where $g(x^*/x)$ is a function of x^* and x alone, and k is independent of x , then X^* is a sufficient statistic for x .

Taking the partial of $\log L$ with respect to x in (B-28) we have

$$\frac{\partial \log L}{\partial x} = \frac{\partial \log g(x^*/x)}{\partial x} \quad (B-29)$$

But (B-24) is a special case of (B-29) where

$$\frac{\partial \log g(x^*/x)}{\partial x} = (B^T A_z^{-1} B + A_x^{-1}) (x^* - x) \quad (B-30)$$

Therefore, whenever (B-20) holds, (B-29) holds also, and X^* is sufficient for estimating x .

UNIQUENESS OF x^*

Since the Likelihood Function L is assumed to be Gaussian or of exponential form, there is only one value of x which maximizes L if the process converges. Since $\partial^2 \log L / \partial x^2 < 0$, every solution of $F(x) = 0$ is a maximum of L . However, by continuity of $\partial^2 \log L / \partial x^2$ there must be a minimum between successive maxima. Since there is no minimum, it follows that there can be no more than one maximum (Reference 12, page 36).

THE WEIGHTED LEAST SQUARES ESTIMATOR x^*

From (B-11) with the a priori values considered as additional observations and the matrices A_x^{-1} and A_z^{-1} regarded as "weighting matrices" for the observations, we seek a solution x^* which minimizes the weighted sum of the squares of the errors from some assumed mathematical model

$$\begin{pmatrix} x \\ f(x) \end{pmatrix}$$

or the minimization of Q which is equivalent to the maximization of L . Hence, under the above assumptions, the Weighted Least Squares Estimator and the Maximum Likelihood Estimator are equivalent.

GLOSSARY AND DEFINITION OF SYMBOLS

Random Vector

Let V_1, V_2, \dots, V_p be p random variables. Then the $(p \times 1)$ vector \mathbf{V} ,

$$\mathbf{V} = \begin{pmatrix} V_1 \\ V_2 \\ \cdot \\ \cdot \\ V_p \end{pmatrix}$$

is a random vector.

Multivariate Normal Distribution

Let the p -dimensional random vector \mathbf{V} have the probability density function

$$|\Omega|^{-1/2} (2\pi)^{-p/2} \exp \left(-\frac{1}{2} (\mathbf{V} - \boldsymbol{\eta})^T \Omega^{-1} (\mathbf{V} - \boldsymbol{\eta}) \right)$$

where $\boldsymbol{\eta}$ is the vector of constants

$$\boldsymbol{\eta} = \begin{pmatrix} \eta_1 \\ \eta_2 \\ \cdot \\ \cdot \\ \eta_p \end{pmatrix}$$

and Ω is a $(p \times p)$ positive definite matrix. Then \mathbf{V} has a nonsingular multivariate normal distribution with mean vector $\mathcal{E}(\mathbf{V}) = \boldsymbol{\eta}$ and covariance matrix

$$\mathcal{E} [(\mathbf{V} - \boldsymbol{\eta})(\mathbf{V} - \boldsymbol{\eta})^T] = \Omega.$$

APPENDIX C

DEFINITION OF COORDINATE SYSTEM AND RADIAL, CROSS TRACK AND DOWN TRACK UNIT VECTORS

THE INERTIAL COORDINATE SYSTEM

The following geocentric coordinate system was used to specify the position and velocity of the satellite at some time or epoch. The fundamental plane is the true equator of the epoch, the x axis points to the vernal equinox of the epoch, the y axis forms a right angle in the equatorial plane, and the z axis is perpendicular to the fundamental plane with the positive direction north. This defines a right-handed orthogonal coordinate system as shown in Figure C-1. This is sometimes called the right ascension declination coordinate system where α is the right ascension and δ is the declination.

RADIAL, CROSS TRACK, AND ALONG TRACK POSITION AND VELOCITY ERRORS

Letting \vec{X}_1 and \vec{X}_2 be the coordinates of the satellite at some time t under two different sets of conditions, the position and velocity vector differences at t in the same coordinate system are given by

$$\vec{\Delta X} = \begin{bmatrix} x_2 - x_1 \\ y_2 - y_1 \\ z_2 - z_1 \end{bmatrix} \quad \vec{\Delta \dot{X}} = \begin{bmatrix} \dot{x}_2 - \dot{x}_1 \\ \dot{y}_2 - \dot{y}_1 \\ \dot{z}_2 - \dot{z}_1 \end{bmatrix} \quad (C-1)$$

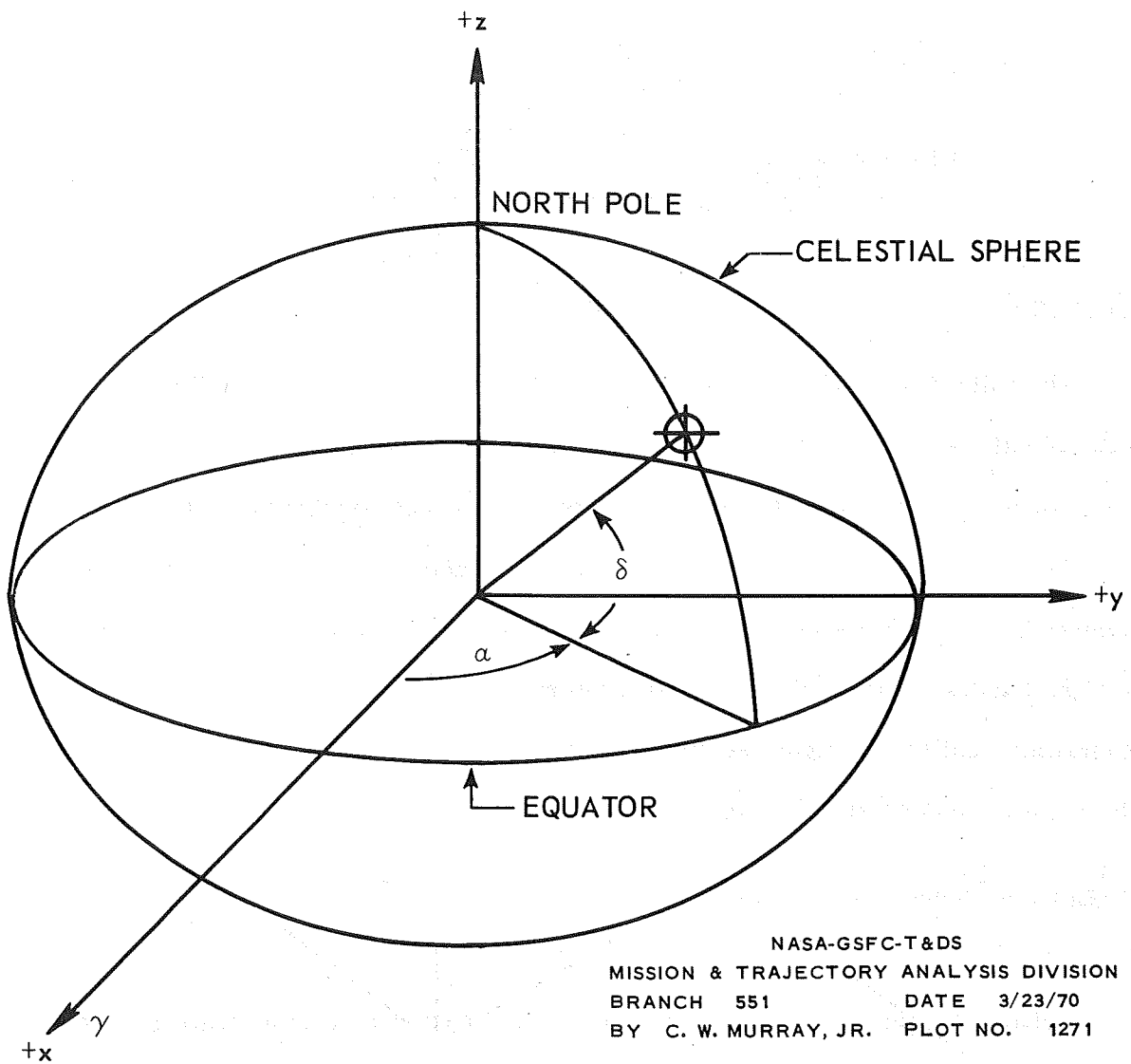
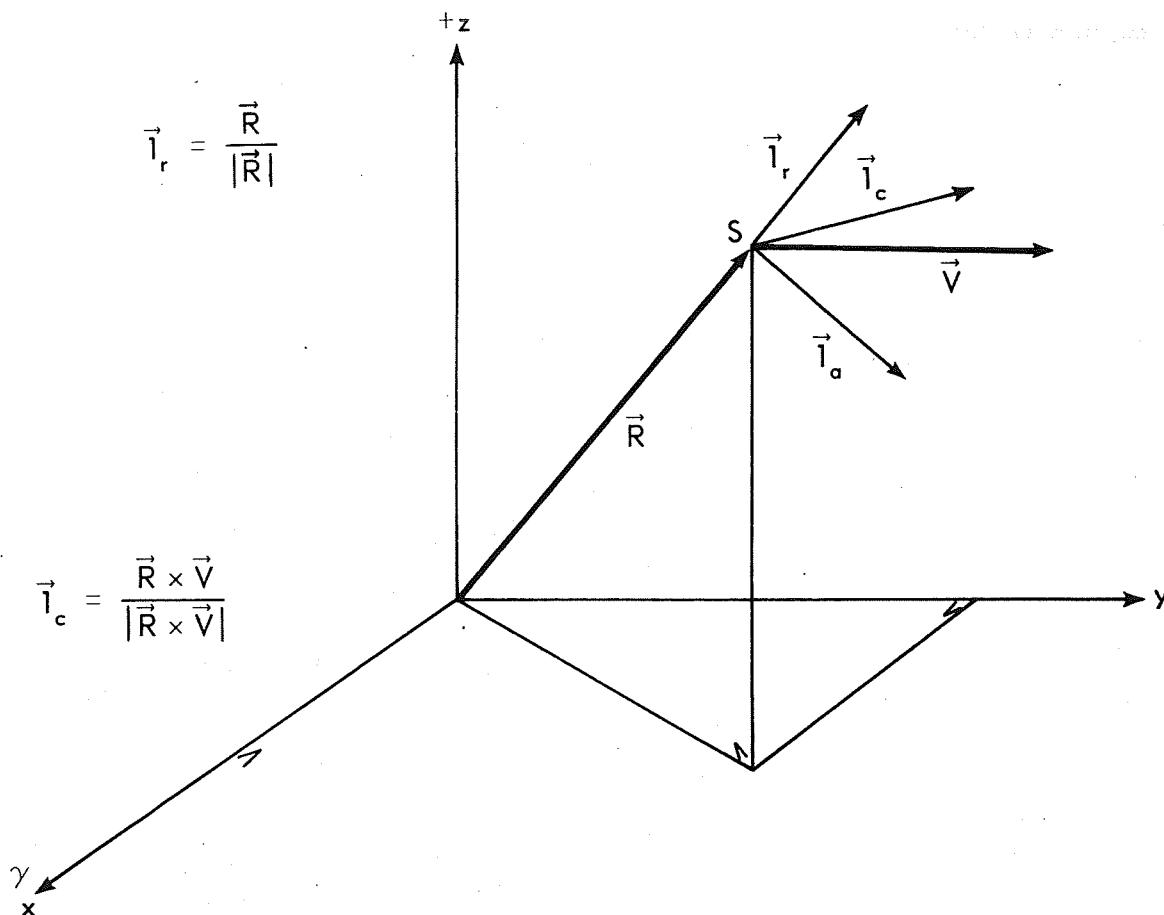


Figure C-1. Inertial Coordinate System

In order to put these differences in the radial, cross track and down track directions consider Figure C-2 where the satellite is located at point S with range vector \vec{R} and velocity vector \vec{V} given by

$$\vec{R} = \begin{bmatrix} x_1 \\ y_1 \\ z_1 \end{bmatrix} \qquad \vec{V} = \begin{bmatrix} \dot{x}_1 \\ \dot{y}_1 \\ \dot{z}_1 \end{bmatrix} \qquad (C-2)$$

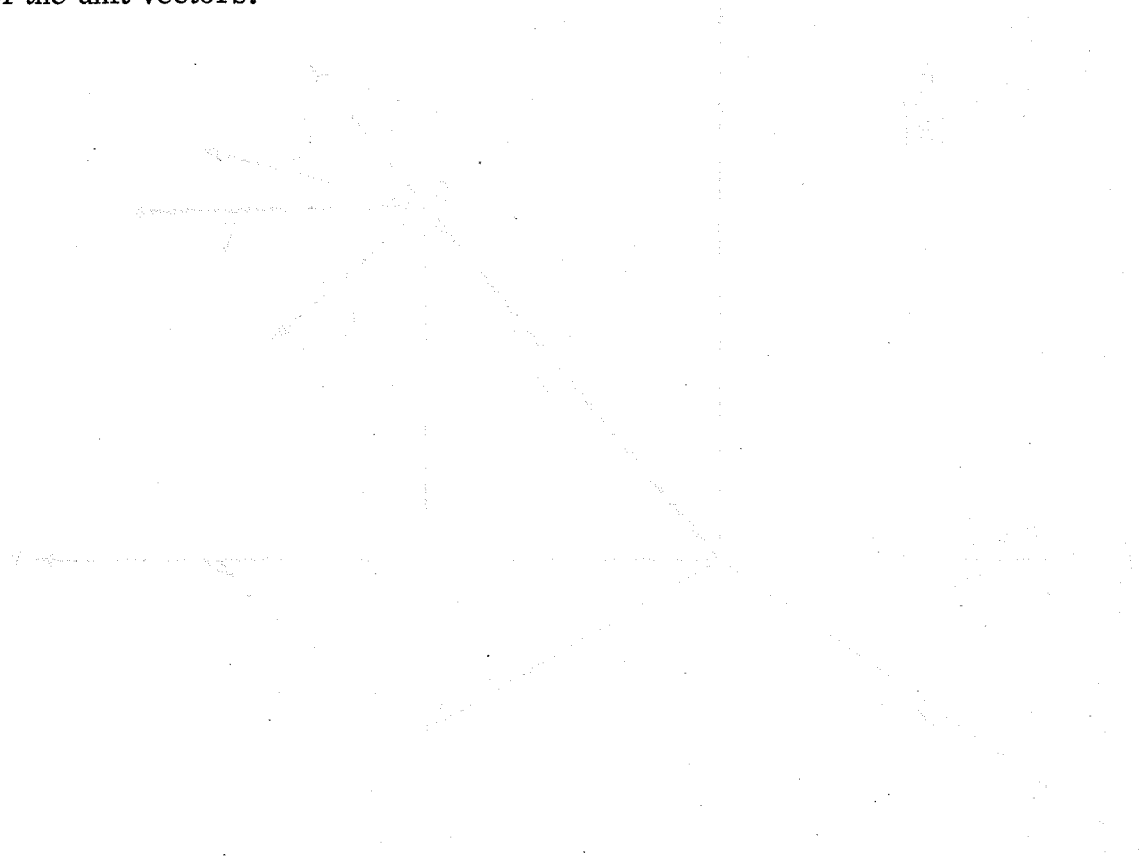
$$\vec{i}_a = \frac{((\vec{R} \times \vec{V}) \times \vec{R})}{|(\vec{R} \times \vec{V}) \times \vec{R}|} = \frac{\vec{V} - \left(\frac{\vec{R} \cdot \vec{V}}{|\vec{R}|^2}\right)\vec{R}}{\sqrt{|\vec{V}|^2 - \left(\frac{\vec{R} \cdot \vec{V}}{|\vec{R}|}\right)^2}}$$



NASA-GSFC-T&DS
 MISSION & TRAJECTORY ANALYSIS DIVISION
 BRANCH 551 DATE 3/23/70
 BY C. W. MURRAY, JR. PLOT NO. 1272

Figure C-2. Radial, Along Track, and Cross Track Unit Vectors In Terms of \vec{R} and \vec{V}

In Figure C-2, the unit vectors in the radial direction, \vec{i}_r , the cross track direction, \vec{i}_c , and the along track (or down track) direction, \vec{i}_a are defined. Then the position differences, will be given by the dot product of ΔX with each of the unit vectors and the velocity differences by the dot product of $\Delta \dot{X}$ with each of the unit vectors.



2025 RELEASE UNDER E.O. 14176